NV5 GEOSPATIAL

January 26, 2023

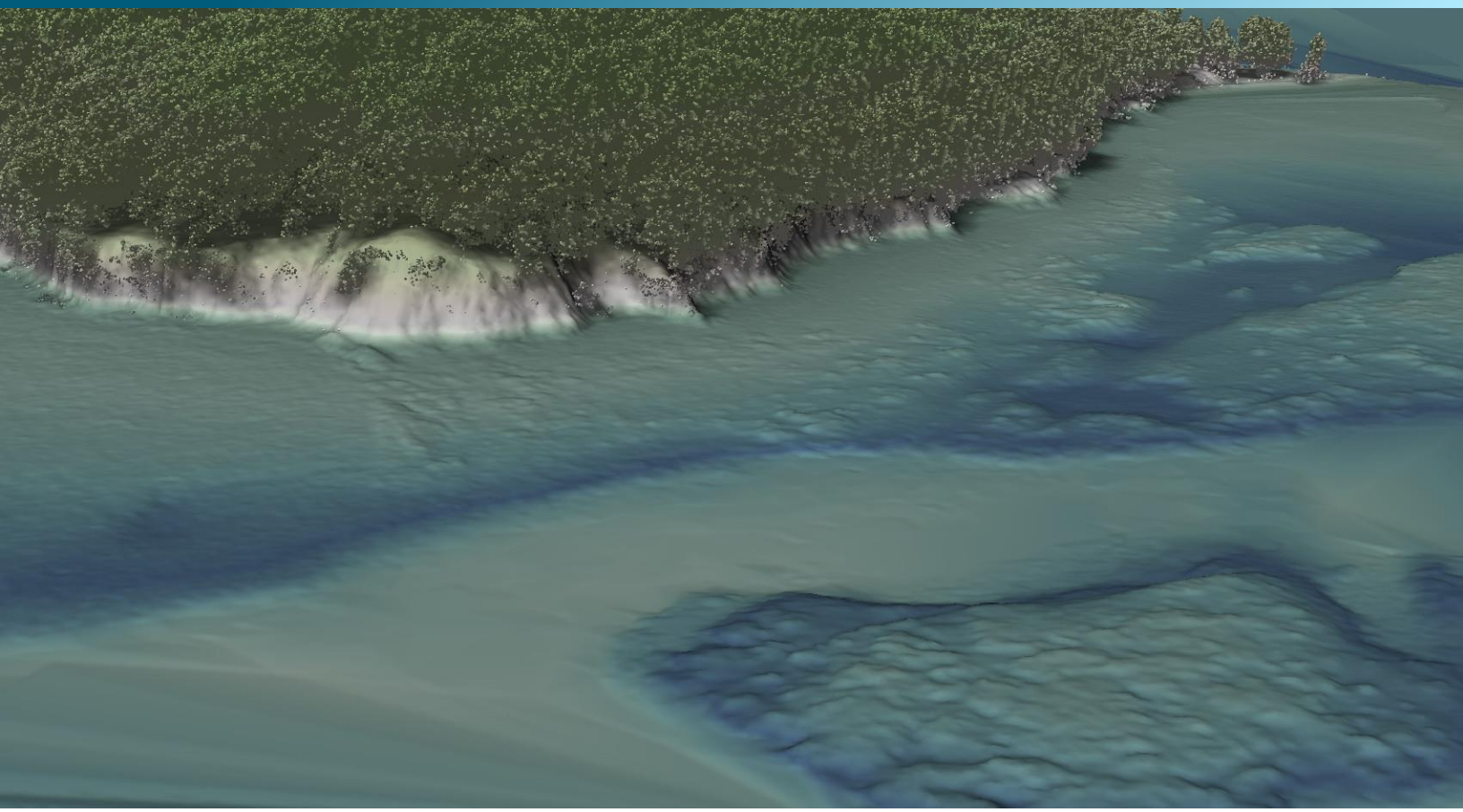

NOAA Finger Lakes, New York

Topobathymetric Lidar Technical Data Report

Prepared For:

NOAA; National Geodetic Survey
Gregory Stinner
1315 East West Hwy
Silver Spring, MD 20910
PH: 240-533-9651

Prepared By:

NV5 Geospatial Corvallis
1100 NE Circle Blvd, Ste. 126
Corvallis, OR 97330
PH: 541-752-1204

TABLE OF CONTENTS

INTRODUCTION 1
Deliverable Products 3
ACQUISITION 5
Airborne Lidar Survey 5
PROCESSING 9
Topobathymetric Lidar Data 9
Lidar Derived Products 12
Topobathymetric DEMs 12
RESULTS & DISCUSSION 13
Bathymetric Lidar 13
Lidar Point Density 13
First Return Point Density 13
Bathymetric and Ground Classified Point Densities 14
Lidar Accuracy Assessments 23
Lidar Non-Vegetated Vertical Accuracy 23
Lidar Relative Vertical Accuracy 26
Lidar Horizontal Accuracy 27
SELECTED IMAGES 28
GLOSSARY 30
APPENDIX A - ACCURACY CONTROLS 31

Cover Photo: A view looking northwest over Lake Champlain. The image was created from the lidar bare earth model overlaid with the above-ground point cloud and colored by elevation.

List of Figures

Figure 1: Location map of the NOAA Finger Lakes sites in New York 4
Figure 2: Ground survey location map for Lake Oneida, Seneca Lake, and Cayuga Lake 7
Figure 3: Ground survey location map for Lake Champlain..... 8
Figure 4: Frequency distribution of first return densities per 100 x 100 m cell..... 15
Figure 5: Frequency distribution of ground and bathymetric bottom classified return densities per 100 x 100 m cell..... 15
Figure 6: First return density map for Oneida Lake in the NOAA Finger Lakes project area (100 m x 100 m cells)..... 16
Figure 7: First return density map for Seneca and Cayuga Lakes in the NOAA Finger Lakes project area (100 m x 100 m cells)..... 17
Figure 8: First return density map for Lake Champlain in the NOAA Finger Lakes project area (100 m x 100 m cells) 18
Figure 9: Ground and bathymetric bottom return density map for Oneida Lake in the NOAA Finger Lakes project area (100 m x 100 m cells) 19
Figure 10: Ground and bathymetric bottom return density map for Seneca Lake in the NOAA Finger Lakes project area (100 m x 100 m cells)..... 20
Figure 11: : Ground and bathymetric bottom return density map for Cayuga Lake in the NOAA Finger Lakes project area (100 m x 100 m cells)..... 21
Figure 12: Ground and bathymetric bottom return density map for Lake Champlain in the NOAA Finger Lakes project area (100 m x 100 m cells)..... 22
Figure 13: Frequency histogram for classified LAS deviation from ground check point values 24
Figure 14: Frequency histogram for lidar bare earth DEM deviation from ground check point values..... 25
Figure 15: Frequency histogram for lidar surface deviation ground control point values 25
Figure 16: Frequency plot for relative vertical accuracy between flight lines 26
Figure 17: View looking west over the Oneida Lake in the NOAA Finger Lakes AOI. The image was created from the lidar bare earth model overlaid with the above-ground point cloud and colored by elevation. 28
Figure 18: View looking northwest over the Seneca Lake in the NOAA Finger Lakes AOI. The image was created from the lidar bare earth model overlaid with the above-ground point cloud and colored by elevation. 28
Figure 19: View looking southwest over the Cayuga Lake in the NOAA Finger Lakes AOI. The image was created from the lidar bare earth model overlaid with the above-ground point cloud and imagery and was colored by elevation. 29
Figure 20: View looking southeast over Lake Champlain in the NOAA Finger Lakes AOI. The image was created from the lidar bare earth model overlaid with the above-ground point cloud and was colored by elevation. 29

List of Tables

Table 1: Acquisition dates, acreage, and data types collected on the NOAA Finger Lakes sites 2
Table 2: Deliverable products coordinate reference system information 3
Table 3: Lidar products delivered for the NOAA Finger Lakes sites 3
Table 4: Lidar specifications and survey settings 6
Table 5: ASPRS LAS classification standards applied to the NOAA Finger Lakes dataset 10
Table 6: Lidar processing workflow 11
Table 7: Average Lidar point densities 14
Table 8: Absolute accuracy results 24
Table 9: Relative accuracy results 26
Table 10: Horizontal Accuracy 27

INTRODUCTION

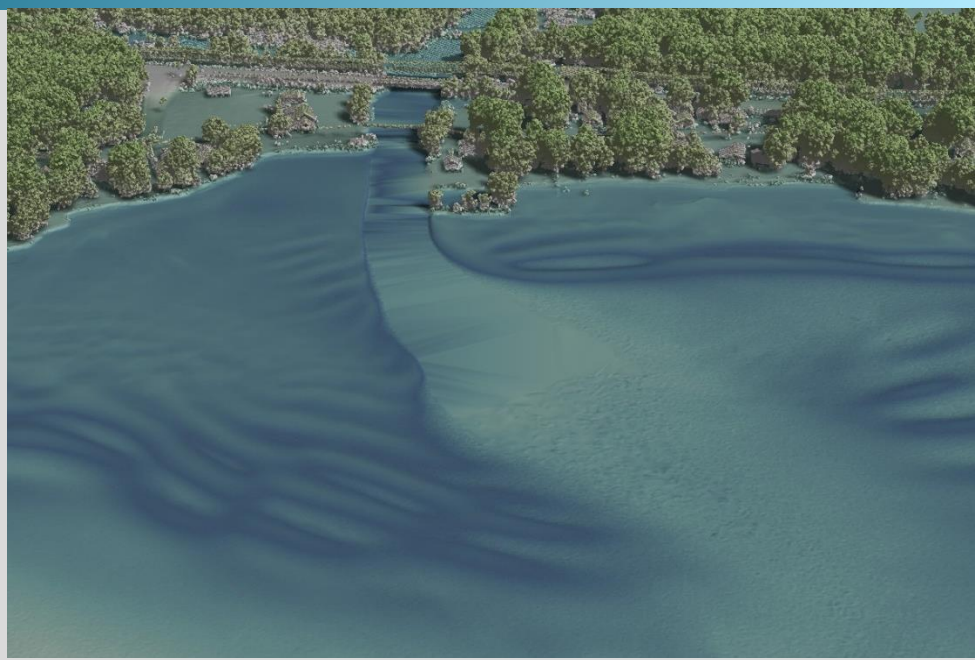

This image looks southeast over the Oneida AOI in the NOAA Finger Lakes project. The image was created from the lidar bare earth model overlaid with the above-ground point cloud and was colored by elevation.

In September to October of 2019, the National Oceanic and Atmospheric Administration (NOAA) acquired topobathymetric lidar data of four lakes. These lakes are located in New York in the Finger Lakes region, with Champlain Lake also extending into Vermont and along the Canadian border. NV5 Geospatial (NV5) was contracted in March 2022 to process and create deliverables out of this data (Contract Number 1305M220DNCNL0064). The NOAA Finger Lakes area of interest was broken into four separate delivery areas, one per lake: Oneida Lake, Seneca Lake, Cayuga Lake, and Lake Champlain. The deliverables will be used to inform and support NOAA's Coastal Mapping Program (CMP) for accurate and consistent shoreline mapping and nautical charting.

This report accompanies the delivered topobathymetric lidar data, and documents contract specifications, data acquisition procedures, processing methods, and analysis of the final dataset including lidar accuracy and lidar point density. Acquisition dates and acreage are shown in, a complete list of contracted deliverables provided to NOAA is shown in Table 3 with the coordinate reference system information for these deliverables shown in Table 2, and the project extent is shown in Figure 1.

Table 1: Acquisition dates, acreage, and data types collected on the NOAA Finger Lakes sites

NOAA project ID	Delivery Area	Buffered Acres	Acquisition Dates	Data Type
NY1908	01: Oneida Lake	54,569	9/25/2019, 9/27/2019, 10/11/2019 – 10/13/2019	Topobathymetric - Lidar
NY1905	02: Seneca Lake	40,544	9/13/2019, 9/15/2019, 9/18/2019	Topobathymetric - Lidar
NY1906	03: Cayuga Lake	52,803	9/19/2019, 9/20/2019, 9/22/2019	Topobathymetric - Lidar
NY2002	04: Lake Champlain	153,234	10/15/2019, 10/19/2019, 10/20/2019, 10/21/2019, 10/22/2019, 10/24/2019, 10/25/2019, 10/26/2019, 10/28/2019, 10/30/2019, 11/06/2019, 11/09/2019	Topobathymetric - Lidar
	Full Project Area	301,150	9/13/2019 – 11/9/2019	Topobathymetric - Lidar

Deliverable Products

Table 2: Deliverable products coordinate reference system information

Projection	Horizontal Datum	Classified LAS Vertical Datum	Raster Model Vertical Datum	Units
UTM Zone 18 North	NAD83(2011)	GRS80 (Ellipsoidal Height)	NAVD88 (Geoid 18)	Meters

Table 3: Lidar products delivered for the NOAA Finger Lakes sites

Product Type	File Type	Product Details
Points	LAS v.1.4 (*.las)	• All Classified Returns
Rasters	1.0 meter Cloud Optimized GeoTiffs	• Bathymetric Void-Clipped Topobathymetric Bare Earth Digital Elevation Model (DEM) • Topobathymetric Standard Deviation Model
Vectors	Shapefiles (*.shp)	• Lidar Tile Index • DEM Tile Index • Delivery Boundary • Bathymetric Void Shape • Delivery Feedback Shape with Response
Metadata	Extensible Markup Language (*.xml)	• LAS Metadata • DEM Metadata
Reports	Adobe Acrobat (*.pdf)	• Lidar Technical Data Report

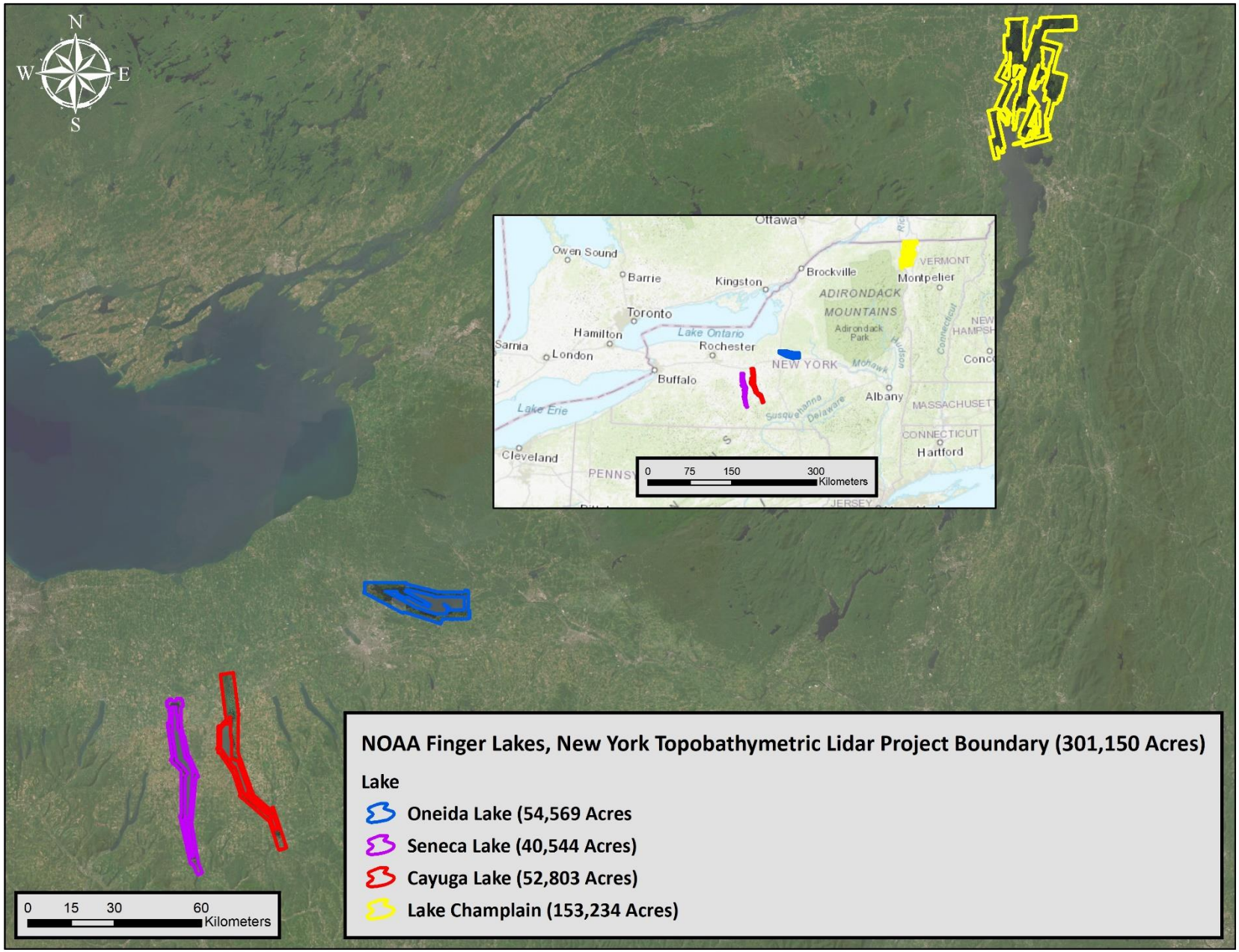

Figure 1: Location map of the NOAA Finger Lakes sites in New York

This image displays a southwest view overlooking the Lake Champlain AOI. The image was created from the lidar bare earth model overlaid with the above-ground point cloud and was colored by elevation.

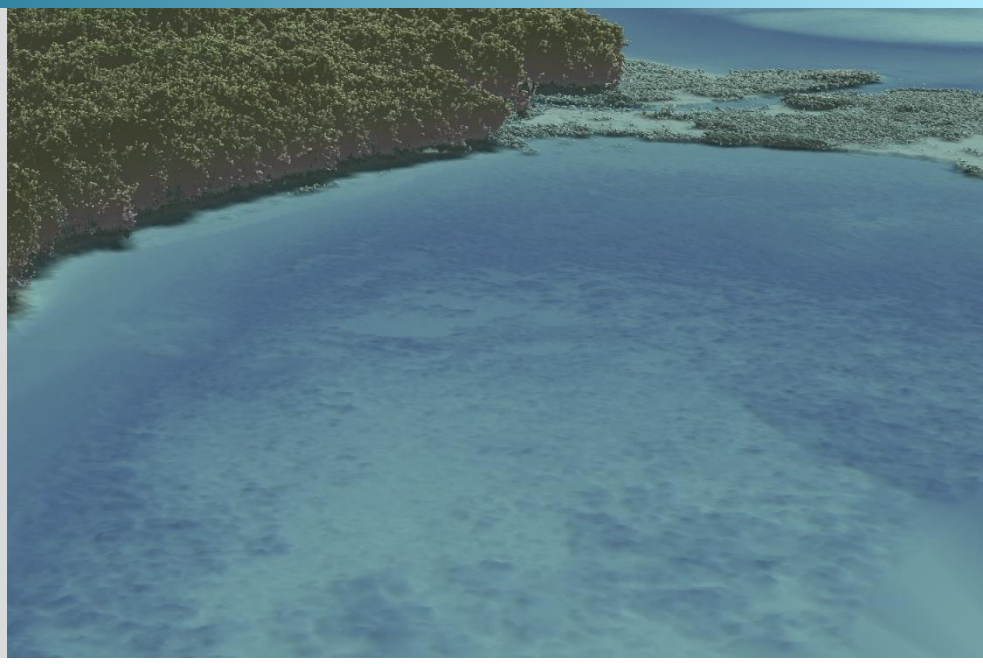

Airborne Lidar Survey

The lidar survey was acquired by NOAA using a Riegl VQ-880-G green laser system mounted in a Twin Otter. The Riegl VQ-880-G boasts a higher repetition pulse rate (up to 550 kHz), higher scanning speed, small laser footprint, and wide field of view which allows for seamless collection of high resolution data of both topographic and bathymetric surfaces. The green wavelength (ʎ=532 nm) laser is capable of collecting high resolution topography data, as well as penetrating the water surface with minimal spectral absorption by water. The Riegl VQ-880-G contains an integrated NIR laser (ʎ=1064 nm) that adds additional topography. Please note that while the Finger Lakes dataset initially provided to NV5 was exclusively green laser data, NOAA provided a small portion of NIR laser data to be integrated into the Cayuga Lake delivery area in order to patch a small, roughly 14 acre datagap in the green dataset. The provided NIR lidar was co-acquired with the Finger Lakes green lidar. The Riegl VQ-880-G laser system can record unlimited range measurements (returns) per pulse, however only a maximum of 15 returns can be stored due to LAS v1.4 file limitations.The recorded waveform enables range measurements for all discernible targets for a given pulse. The number of returns digitized from a single pulse ranged from 1 to 7 in the NOAA Finger Lakes project dataset. It is not uncommon for some types of surfaces (e.g., dense vegetation or water) to return fewer pulses to the lidar sensor than the laser originally emitted. The discrepancy between first return and overall delivered density will vary depending on terrain, land cover, and the prevalence of water bodies. All discernible laser returns were processed for the output dataset. Table 4 summarizes the settings used to yield an average pulse density of ≥9 pulses/m^2 over the NOAA Finger Lakes project area.

Table 4: Lidar specifications and survey settings

Parameter	Green Laser	NIR Laser
Acquisition Dates	9/13/2019 – 11/09/2019	9/20/2019
Aircraft Used	NOAA Twin Otter	NOAA Twin Otter
Sensor	Riegl	Riegl
Laser	VQ 880G-Green	VQ-880G-IR
Maximum Returns	7	7
Resolution/Density	Average 9 pulses/m^2	Average 9 pulses/m^2
Nominal Pulse Spacing	0.33 m	0.33 m
Survey Altitude (AGL)	396 m (1300 ft)	396 m (1300 ft)
Survey speed	100 knots	100 knots
Field of View	40°	40°
Mirror Scan Rate	80 Lines per Second	Uniform Point Spacing
Target Pulse Rate	145 kHz	145 kHz
Pulse Length	1.5 ns	3 ns
Laser Pulse Footprint Diameter	27 - 79 cm	8 cm
Central Wavelength	532 nm	1064 nm
Pulse Mode	Multiple Times Around	Multiple Times Around
Beam Divergence	0.7 - 2.0 mrad	0.2 mrad
Swath Width	288 m	288 m
Swath Overlap	50%	50%
Intensity	16-bit	16-bit

Ground Survey

NOAA performed the ground survey data collection for the Finger Lakes project. The ground survey data was provided to NV5 to perfom quality assurance checks and assess the lidar accuracy. NOAA utilized post processed kinematic (PPK) survey techniques to collect the ground survey points and base stations (Figure 2 and Figure 3). PPK surveys compute corrections from a base station or Real-Time Network (RTN) during post-processing to achieve a high level of accuracy. PPK surveys record data while stationary for at least five seconds, calculating the position using at least three one-second epochs.

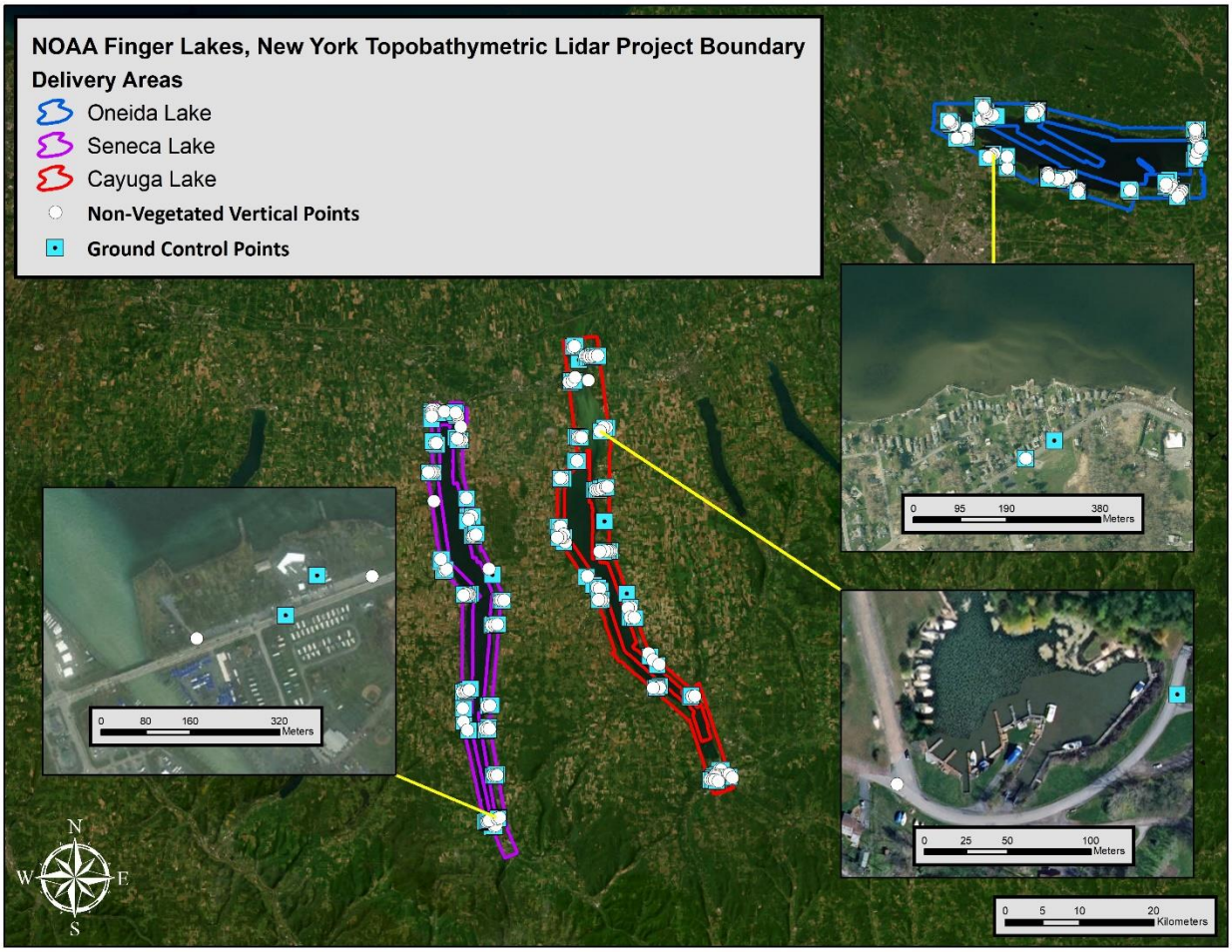

Figure 2: Ground survey location map for Lake Oneida, Seneca Lake, and Cayuga Lake in the NOAA Finger Lakes AOI

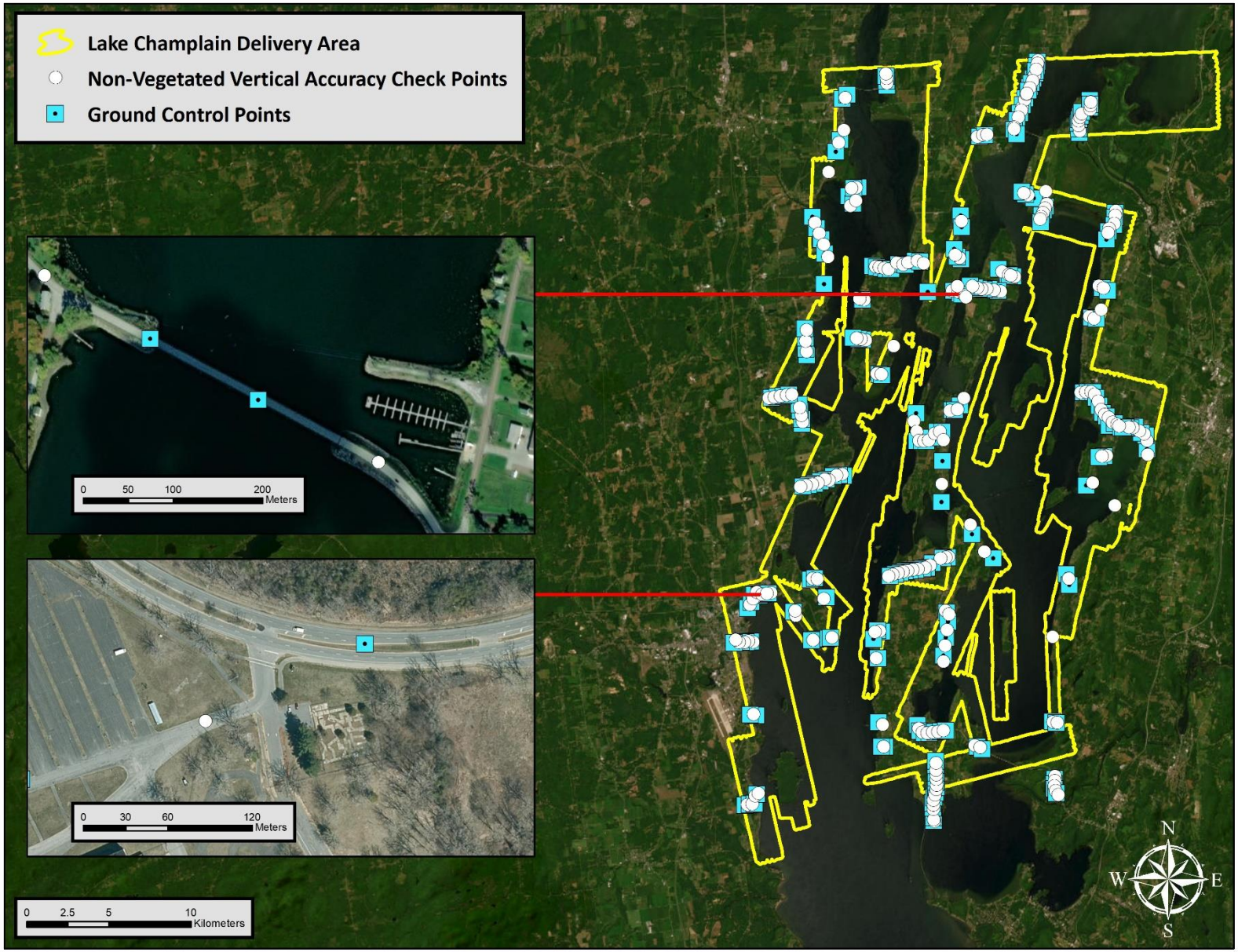

Figure 3: Ground survey location map for Lake Champlain

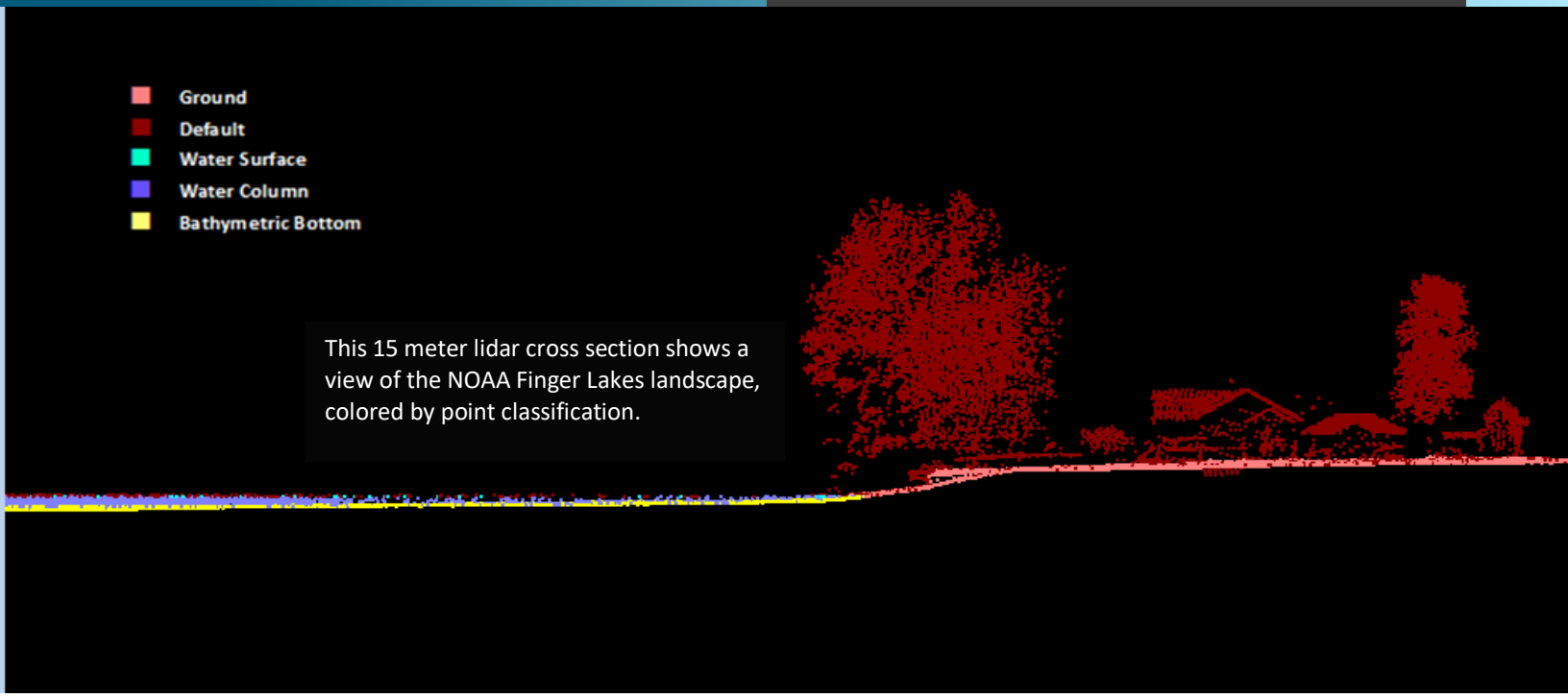

This 15 meter lidar cross section shows a view of the NOAA Finger Lakes landscape, colored by point classification.

Topobathymetric Lidar Data

NOAA acquired, extracted, refracted, and calibrated the Finger Lakes topobathymetric lidar data. SBETs, ground survey data, and raw LAS files were generated by NOAA and provided to NV5 in order to calculate accuracies and densities, and produce product deliverables including a classified point cloud. (Table 5). Processing methodologies were tailored specifically for the project area's landscape. Brief descriptions of these tasks are shown in Table 6.

Table 5: ASPRS LAS classification standards applied to the NOAA Finger Lakes dataset

Classification Number	Classification Name	Classification Description
1	Unclassified	Processed, but unclassified
2	Ground	Bare-earth ground
7 Withheld	Low Noise	Noise (low manually identified)
18 Withheld	High Noise	Noise (high manually identified)
40	Bathymetric Bottom	Bathymetric point (e.g., seafloor or riverbed; also known as submerged topography)
41	Water Surface	Water's surface (sea/river/lake surface from topographic-bathymetric lidar.
43	Submerged Feature	Submerged object, not otherwise specified (e.g., wreck, rock, submerged piling)
44	S-57 Object	International Hydrographic Organization (IHO) S-57 object, not otherwise specified
45	Water Column	Refracted returns not determined to be water surface or bathymetric bottom
64	Submerged Aquatic Vegetation	Benthic vegetation in submerged, refracted areas
65	Overlap Bathymetric Bottom	Denotes bathymetric bottom temporal changes from varying lifts, not utilized in bathymetric point class
1-Withheld	Edge Clip	Unclassified points flagged as withheld. These are primarily "edge" points from the higher scan angle being removed.

Table 6: Lidar processing workflow

Lidar Processing Step	Software Used
NOAA extracted, refracted, and created smoothed best estimate of trajectories (SBET) and the raw unclassified LAS point cloud.	POSPac MMS RiProcess GeoCue TerraSolid
NV5 classified resulting data to ground and other client-designated ASPRS classifications (Table 5). NV5 assessed statistical absolute accuracy via direct comparisons of ground classified points to ground control survey data.	TerraScan TerraModeler
NV5 generated bare earth models as triangulated surfaces to create cloud optimized GeoTiffs at a 1.0 meter pixel resolution.	TerraScan TerraModeler Las Product Creator (NV5 proprietary software) ArcMap

Lidar Derived Products

Because hydrographic laser scanners penetrate the water surface to map submerged topography, this affects how the data should be processed and presented in derived products from the lidar point cloud. The following section discusses certain derived products that vary from the traditional (NIR) specification and delivery format.

Topobathymetric DEMs

Bathymetric bottom returns can be limited by depth, water clarity, and bottom surface reflectivity. Water clarity and turbidity affects the depth penetration capability of the green wavelength laser with returning laser energy diminishing by scattering throughout the water column. Additionally, the bottom surface must be reflective enough to return remaining laser energy back to the sensor at a detectable level. Although the predicted depth penetration range of the Riegl VQ-880-G sensor is 1.5 Secchi depths on brightly reflective surfaces, it is not unexpected to have no bathymetric bottom returns in turbid or non-reflective areas.

As a result, creating digital elevation models (DEMs) presents a challenge with respect to interpolation of areas with no returns. Traditional DEMs are “unclipped”, meaning areas lacking ground returns are interpolated from neighboring ground returns (or breaklines in the case of hydro-flattening), with the assumption that the interpolation is close to reality. In bathymetric modeling, these assumptions are prone to error because a lack of bathymetric returns can indicate a change in elevation that the laser can no longer map due to increased depths. The resulting void areas may suggest greater depths, rather than similar elevations from neighboring bathymetric bottom returns. Therefore, NV5 created a bathymetric void polygon to delineate areas without mapped bathymetry within the Finger Lakes project boundary. This shapefile was used to control the extent of the delivered bathymetric void-clipped topobathymetric models to avoid false triangulation (interpolation from TIN’ing) across refracted areas without bathymetric bottom returns.

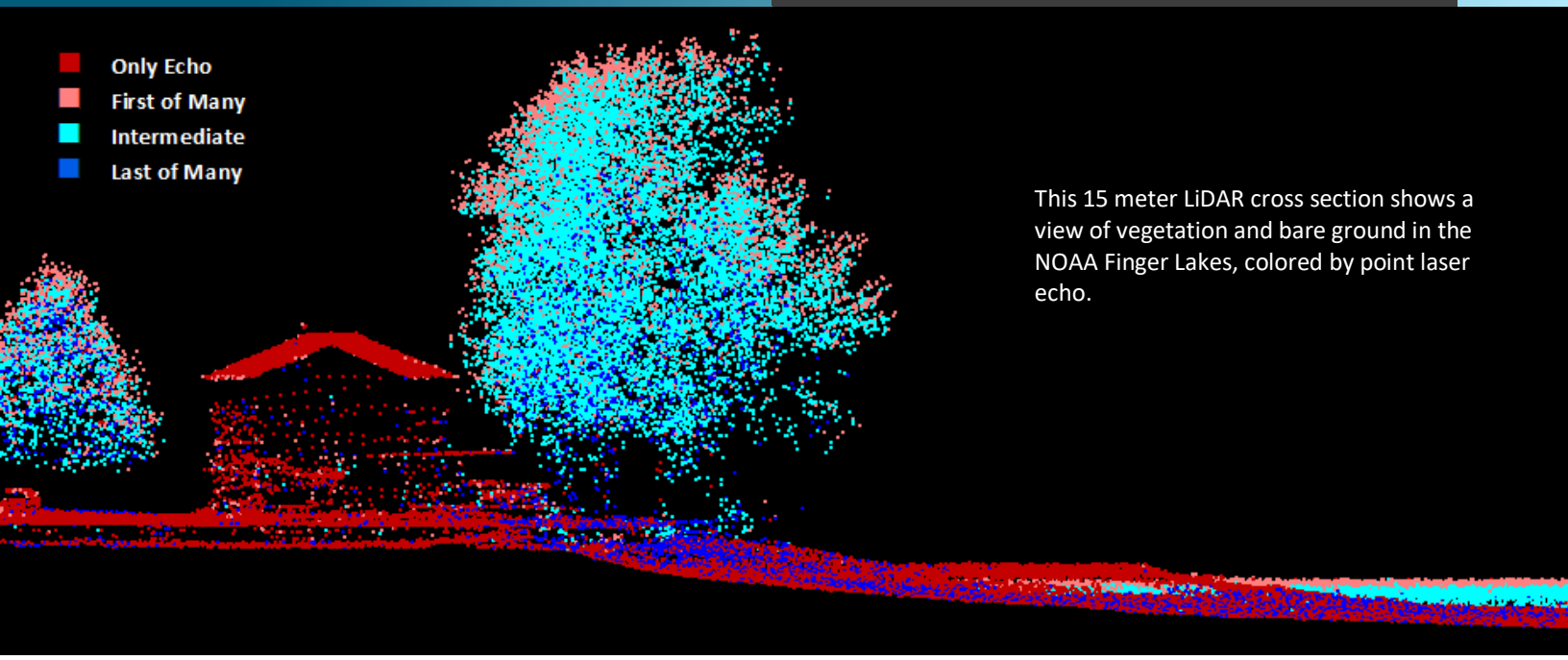

This 15 meter LiDAR cross section shows a view of vegetation and bare ground in the NOAA Finger Lakes, colored by point laser echo.

Bathymetric Lidar

An underlying principle for collecting hydrographic lidar data is to survey near-shore areas that can be difficult to collect with other methods, such as multi-beam sonar, particularly over large areas. The capability and effectiveness of the bathymetric lidar is impacted by several parameters including depth penetrations below the water surface, bathymetric return density, and spatial accuracy.

Lidar Point Density

First Return Point Density

The acquisition parameters were designed to acquire an average first-return density of 9 points/m^2. First return density describes the density of pulses emitted from the laser that return at least one echo to the system. Multiple returns from a single pulse were not considered in first return density analysis. Some types of surfaces (e.g., breaks in terrain, water and steep slopes) may have returned fewer pulses than originally emitted by the laser.

First returns typically reflect off the highest feature on the landscape within the footprint of the pulse. In forested or urban areas the highest feature could be a tree, building or power line, while in areas of unobstructed ground, the first return will be the only echo and represents the bare earth surface.

The average first-return density of the NOAA Finger Lakes Lidar project was 12.50 points/ m^2 (Table 7). The statistical and spatial distributions of all first return densities per 100 m x 100 m cell are portrayed in Figure 4 and Figure 6 through Figure 8.

Bathymetric and Ground Classified Point Densities

The density of ground classified lidar returns and bathymetric bottom returns were also analyzed for this project. Terrain character, land cover, and ground surface reflectivity all influenced the density of ground surface returns. In vegetated areas, fewer pulses may have penetrated the canopy, resulting in lower ground density. Similarly, the density of bathymetric bottom returns was influenced by turbidity, depth, and bottom surface reflectivity. In turbid areas, fewer pulses may have penetrated the water surface, resulting in lower bathymetric density.

The ground and bathymetric bottom classified density of lidar data for the NOAA Finger Lakes project was 3.25 points/m^2(Table 7). The statistical and spatial distributions ground classified and bathymetric bottom return densities per 100 m x 100 m cell are portrayed in Figure 5 and Figure 9 through Figure 12.

Table 7: Average Lidar point densities

Density Type	Point Density
First Returns	12.50 points/m²
Ground and Bathymetric Bottom Classified Returns	3.25 points/m²

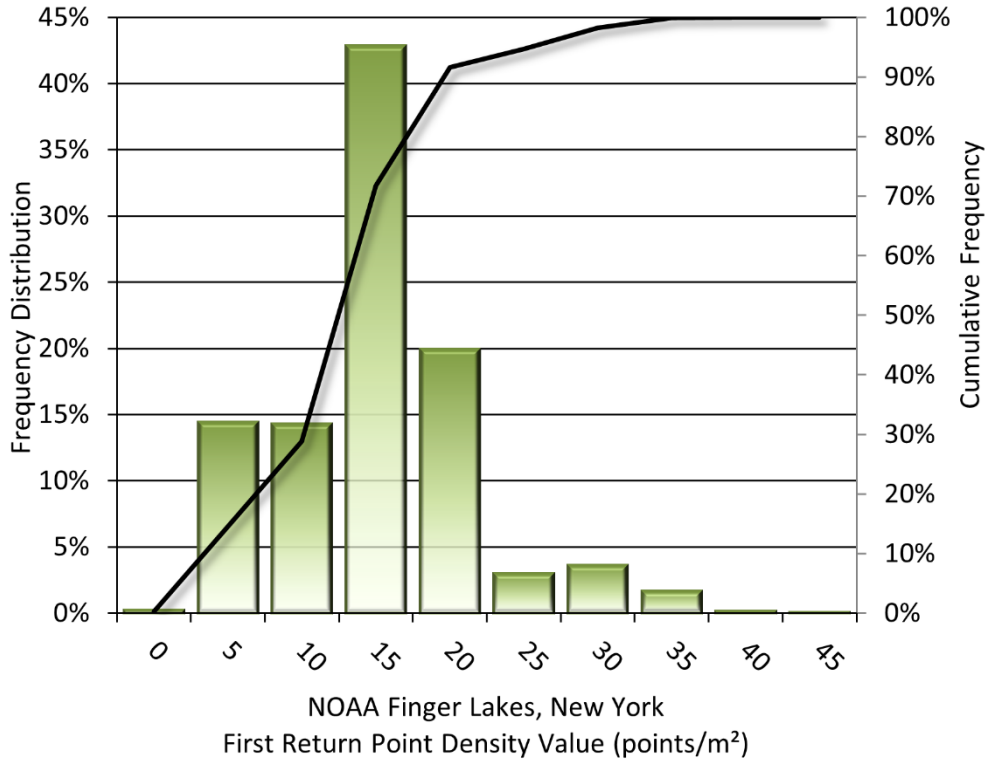

Figure 4: Frequency distribution of first return densities per 100 x 100 m cell

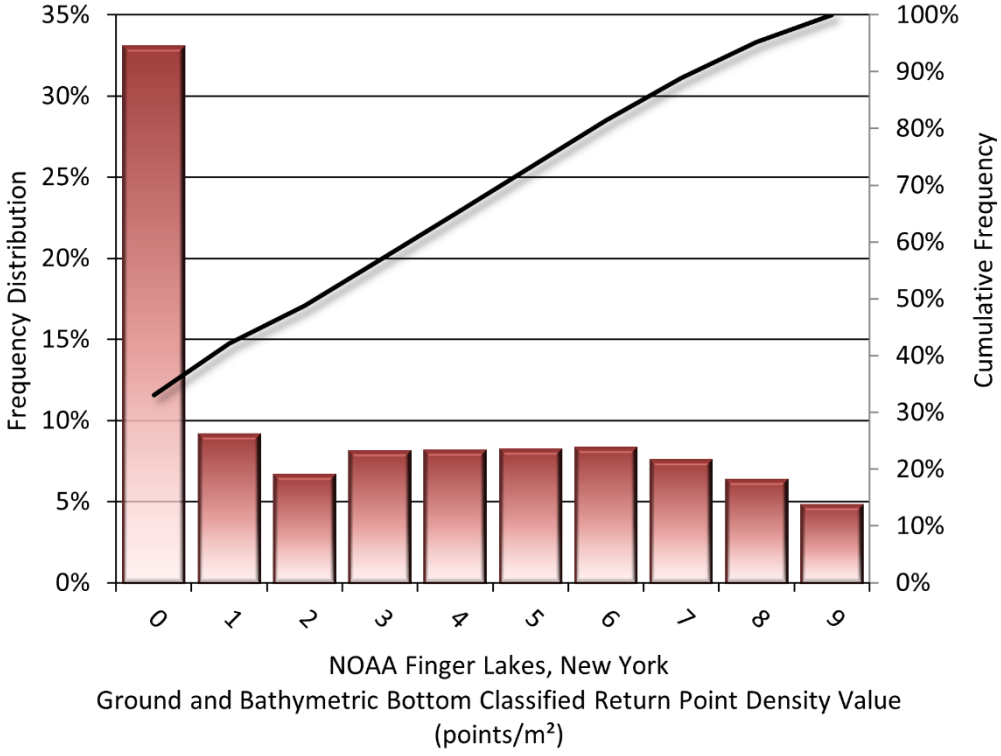

Figure 5: Frequency distribution of ground and bathymetric bottom classified return densities per 100 x 100 m cell

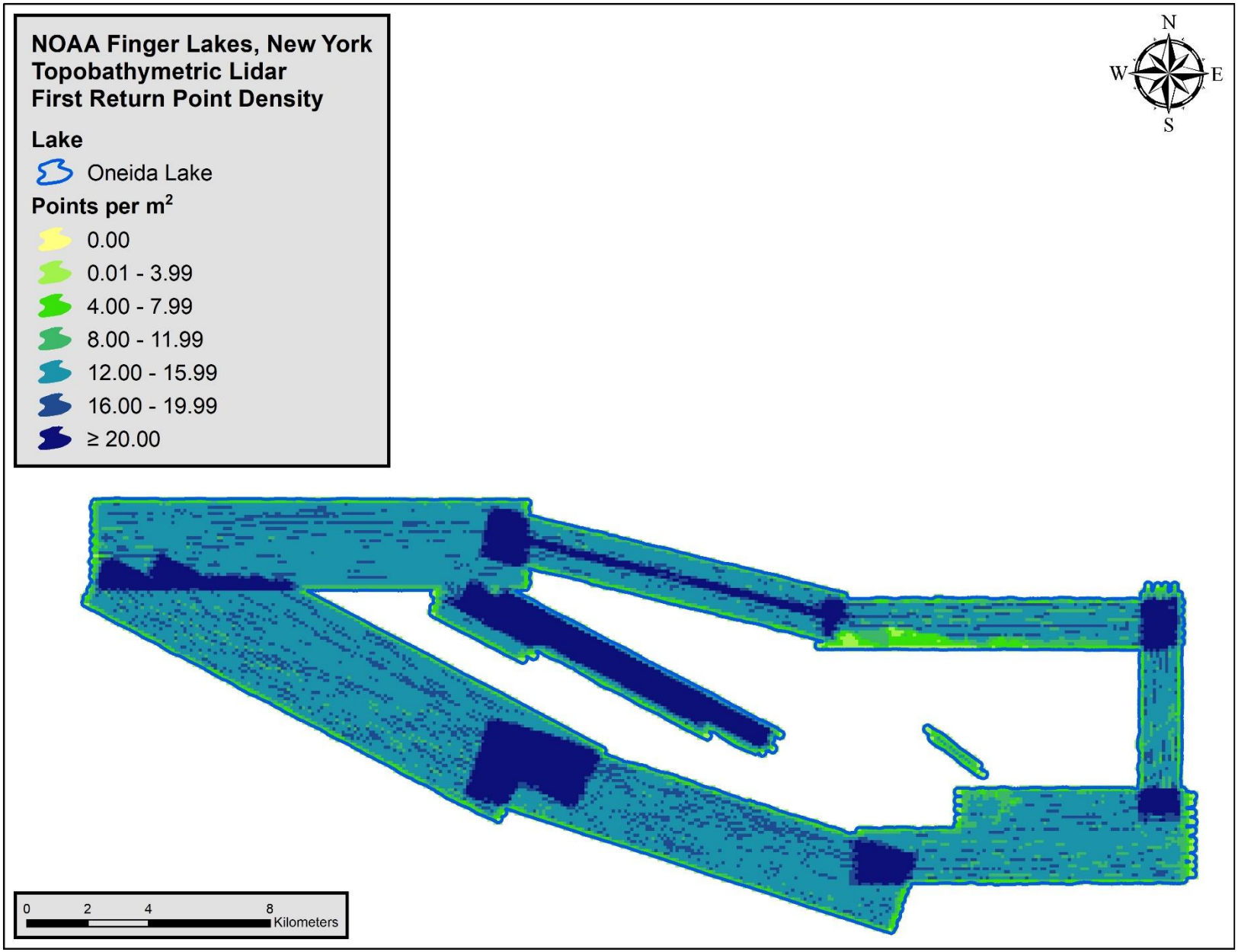

Figure 6: First return density map for Oneida Lake in the NOAA Finger Lakes project area (100 m x 100 m cells)

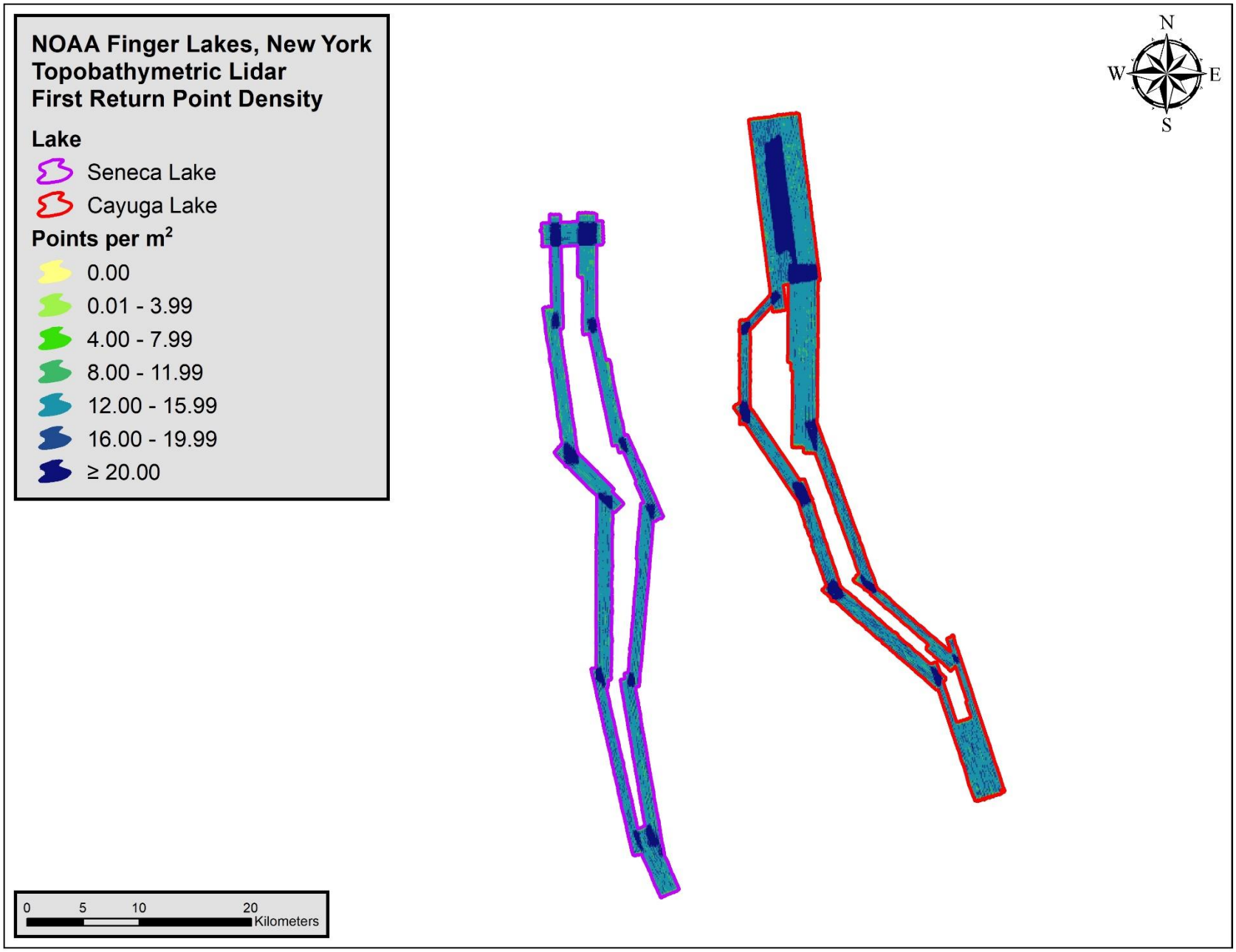

Figure 7: First return density map for Seneca and Cayuga Lakes in the NOAA Finger Lakes project area (100 m x 100 m cells)

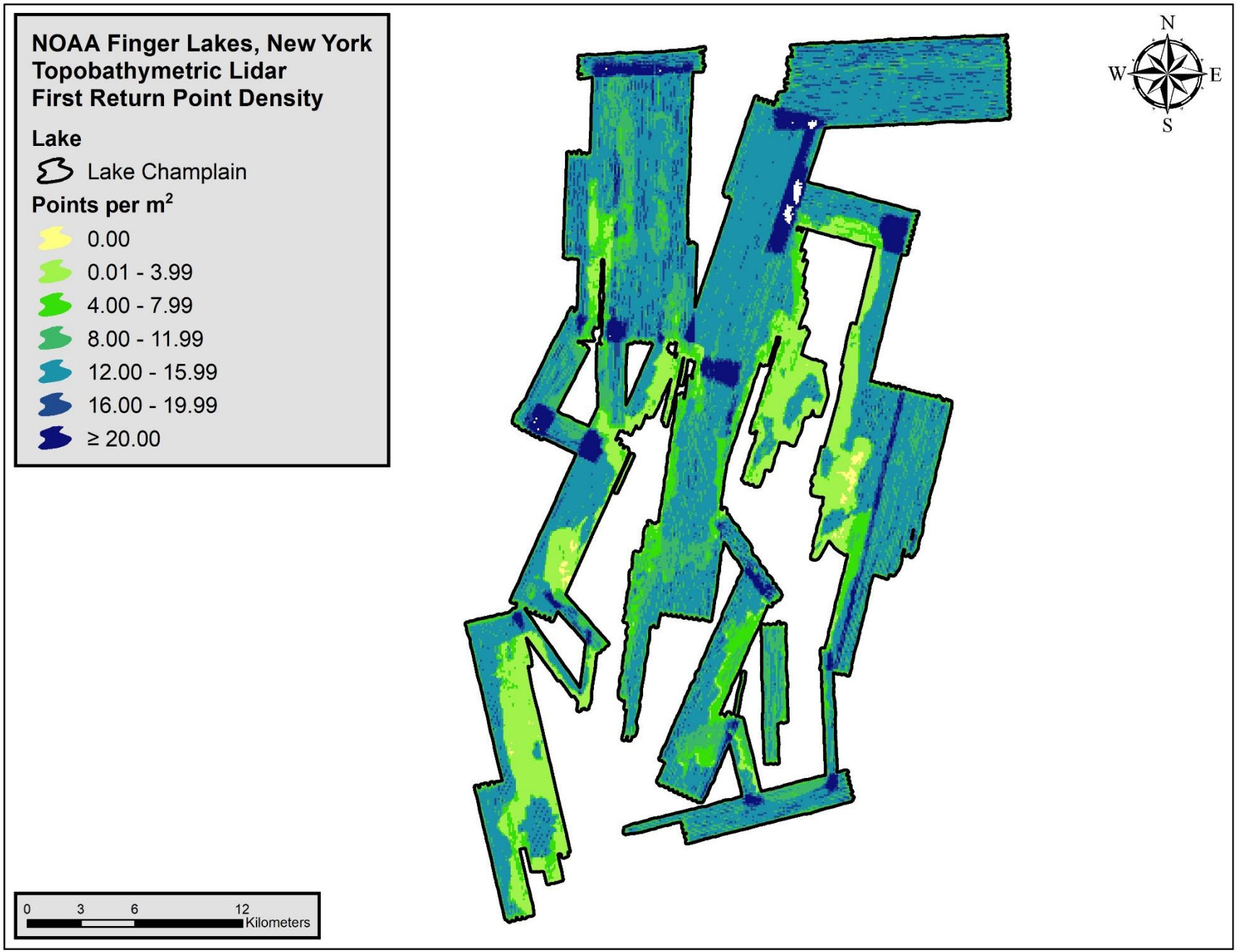

Figure 8: First return density map for Lake Champlain in the NOAA Finger Lakes project area (100 m x 100 m cells)

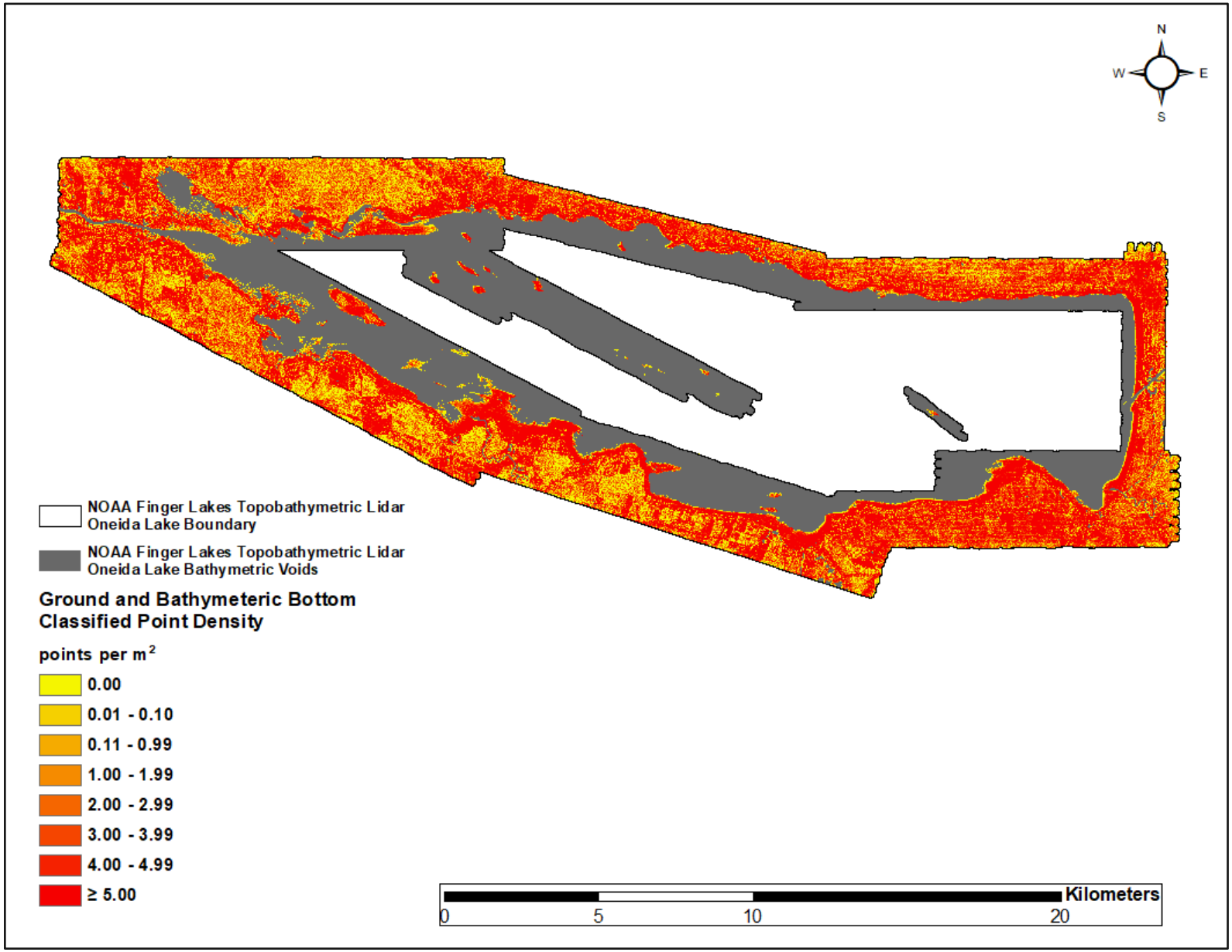

Figure 9: Ground and bathymetric bottom return density map for Oneida Lake in the NOAA Finger Lakes project area (100 m x 100 m cells)

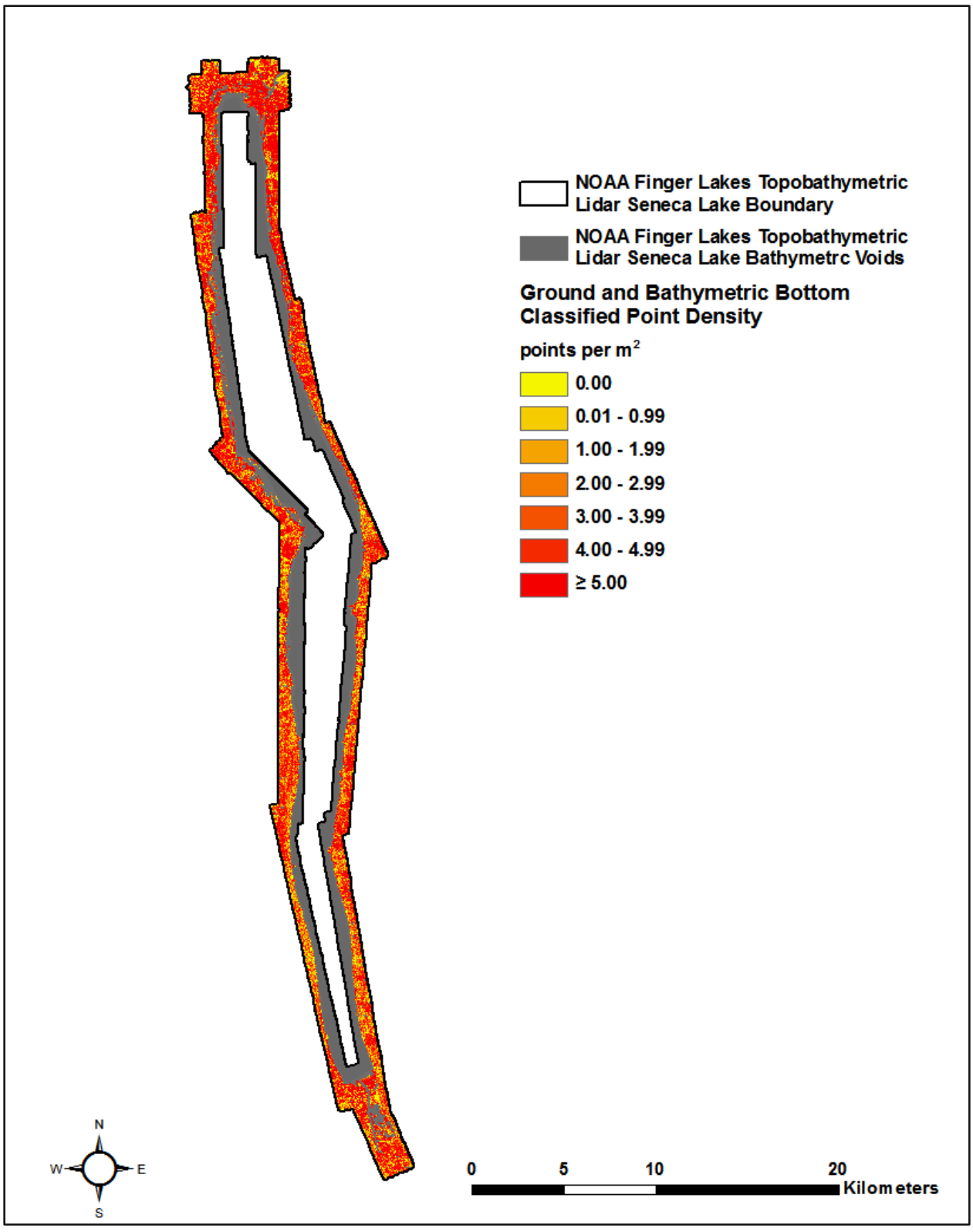

Figure 10: Ground and bathymetric bottom return density map for Seneca Lake in the NOAA Finger Lakes project area (100 m x 100 m cells)

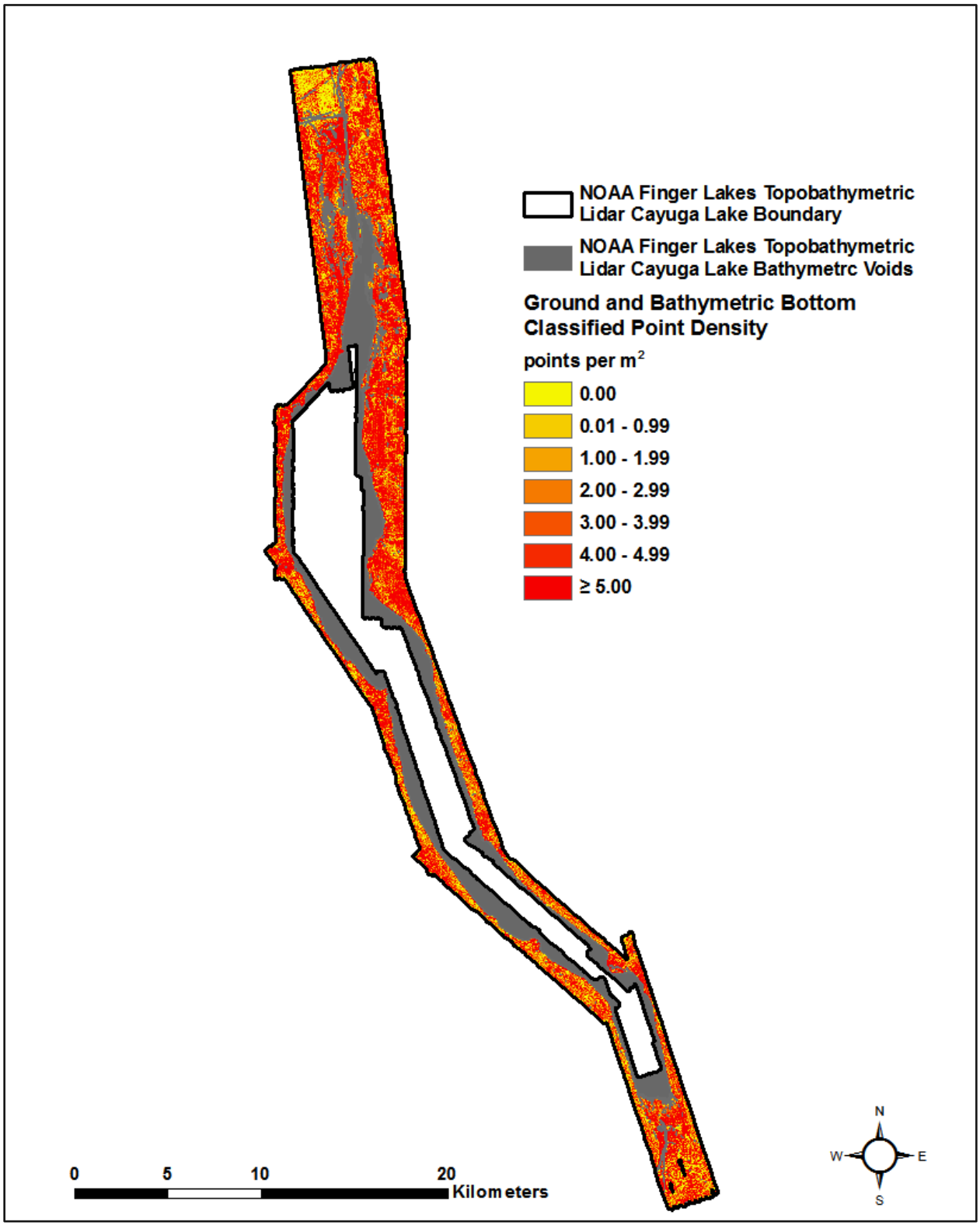

Figure 11: : Ground and bathymetric bottom return density map for Cayuga Lake in the NOAA Finger Lakes project area (100 m x 100 m cells)

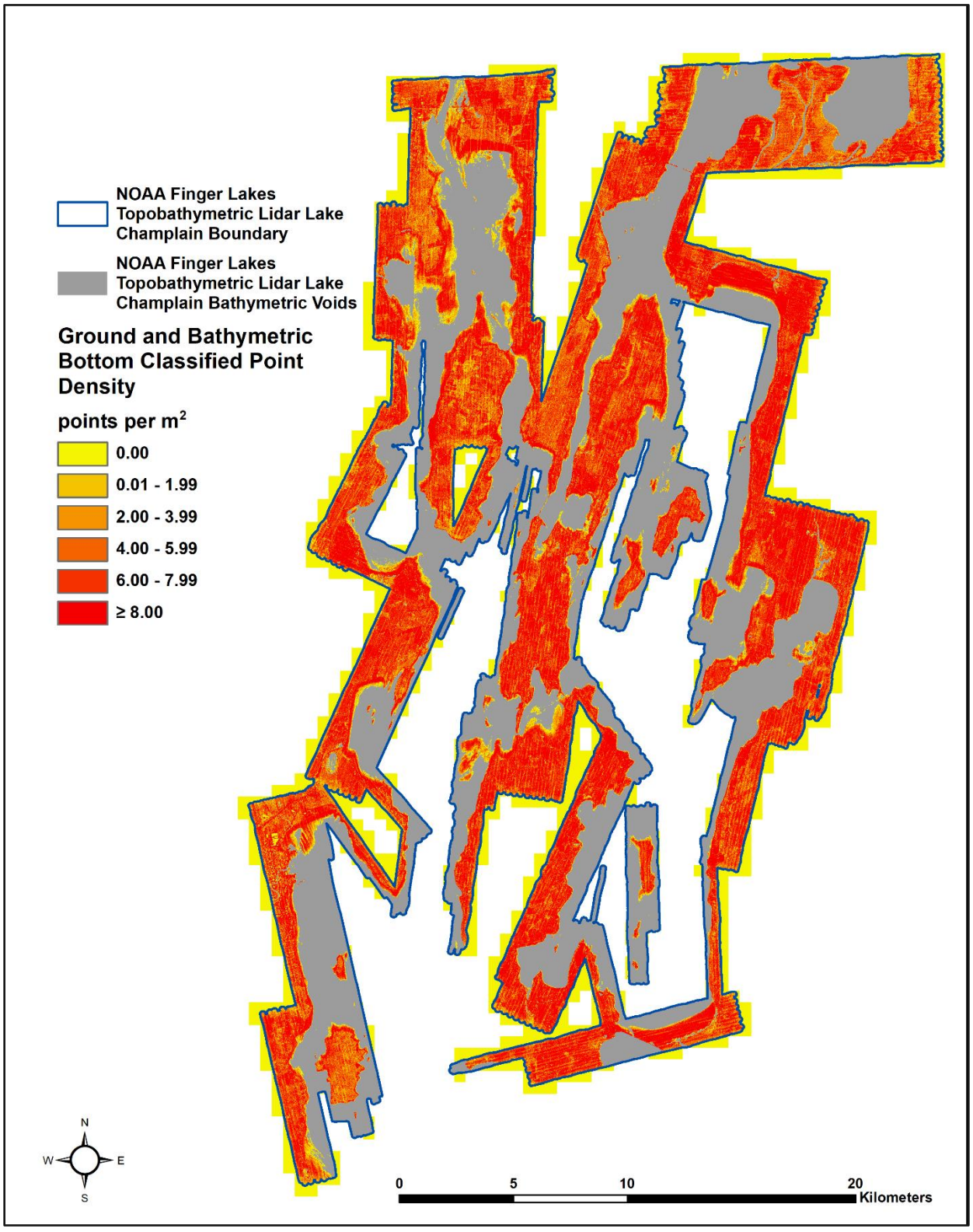

Figure 12: Ground and bathymetric bottom return density map for Lake Champlain in the NOAA Finger Lakes project area (100 m x 100 m cells)

Lidar Accuracy Assessments

The accuracy of the lidar data collection can be described in terms of absolute accuracy (the consistency of the data with external data sources) and relative accuracy (the consistency of the dataset with itself). See Appendix A for further information on sources of error and operational measures used to improve relative accuracy.

Lidar Non-Vegetated Vertical Accuracy

Absolute accuracy was assessed using Non-vegetated Vertical Accuracy (NVA) reporting designed to meet guidelines presented in the FGDC National Standard for Spatial Data Accuracy[1]. NVA compares known ground check point data that were withheld from the calibration and post-processing of the lidar point cloud to the triangulated surface generated by the classified lidar point cloud as well as the derived gridded bare earth DEM. NVA is a measure of the accuracy of lidar point data in open areas where the lidar system has a high probability of measuring the ground surface and is evaluated at the 95% confidence interval (1.96 * RMSE), as shown in Table 8.

The mean and standard deviation (sigma σ) of divergence of the ground surface model from ground check point coordinates are also considered during accuracy assessment. These statistics assume the error for x, y and z is normally distributed, and therefore the skew and kurtosis of distributions are also considered when evaluating error statistics. For the NOAA Finger Lakes survey, 400 ground check points were withheld from the calibration and post-processing of the lidar point cloud, with resulting non-vegetated vertical accuracy of 0.081 meters, as compared to the classified LAS and 0.093 meters against the bare earth DEM, with 95% confidence (Figure 13 and Figure 14).

NV5 also assessed absolute accuracy using 402 ground control points. Although these points were used in the calibration and post-processing of the lidar point cloud, they still provide a good indication of the overall accuracy of the lidar dataset, and therefore have been provided in Table 8 and Figure 15.

[1] Federal Geographic Data Committee, ASPRS POSITIONAL ACCURACY STANDARDS FOR DIGITAL GEOSPATIAL DATA EDITION 1, Version 1.0, NOVEMBER 2014. https://www.asprs.org/a/society/committees/standards/Positional_Accuracy_Standards.pdf.

Table 8: Absolute accuracy results

Parameter	NVA, as compared to Classified LAS	NVA, as compared to Bare Earth DEM	Ground Control Points
Sample	400 points	400 points	402 points
95% Confidence (1.96*RMSE)	0.081 m	0.093 m	0.091 m
Average	0.003 m	0.002 m	0.000 m
Median	0.007 m	0.004 m	-0.002 m
RMSE	0.041 m	0.047 m	0.046 m
Standard Deviation (1σ)	0.041 m	0.047 m	0.046 m

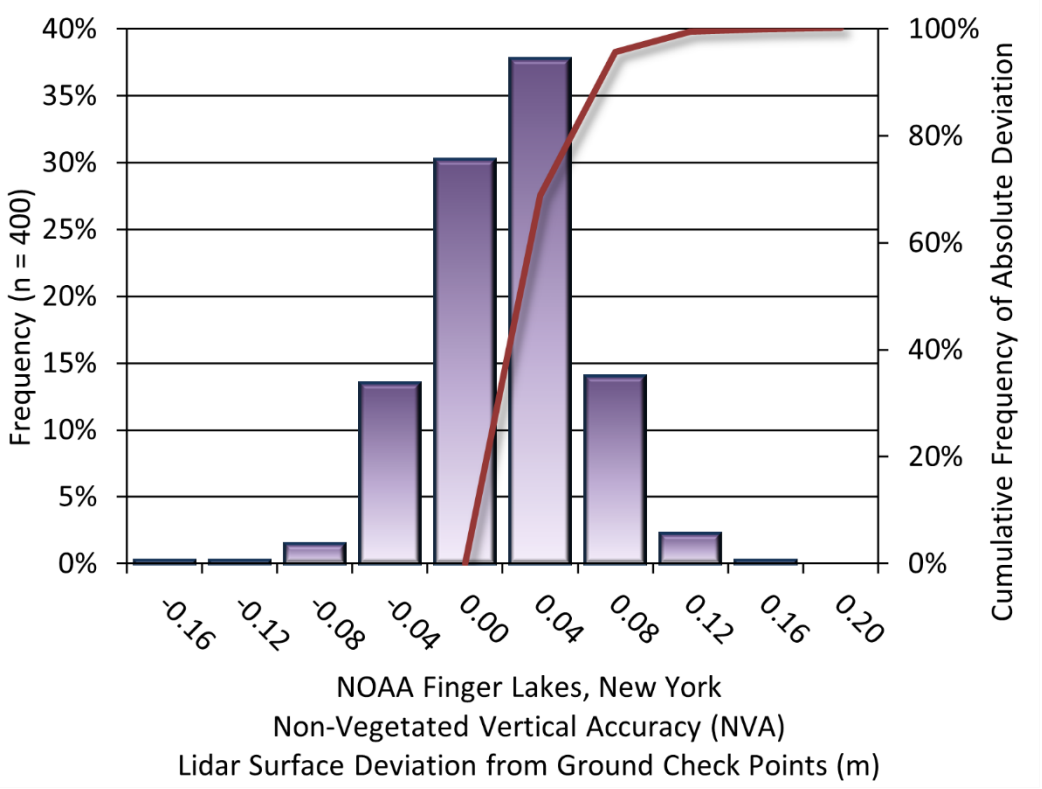

Figure 13: Frequency histogram for classified LAS deviation from ground check point values

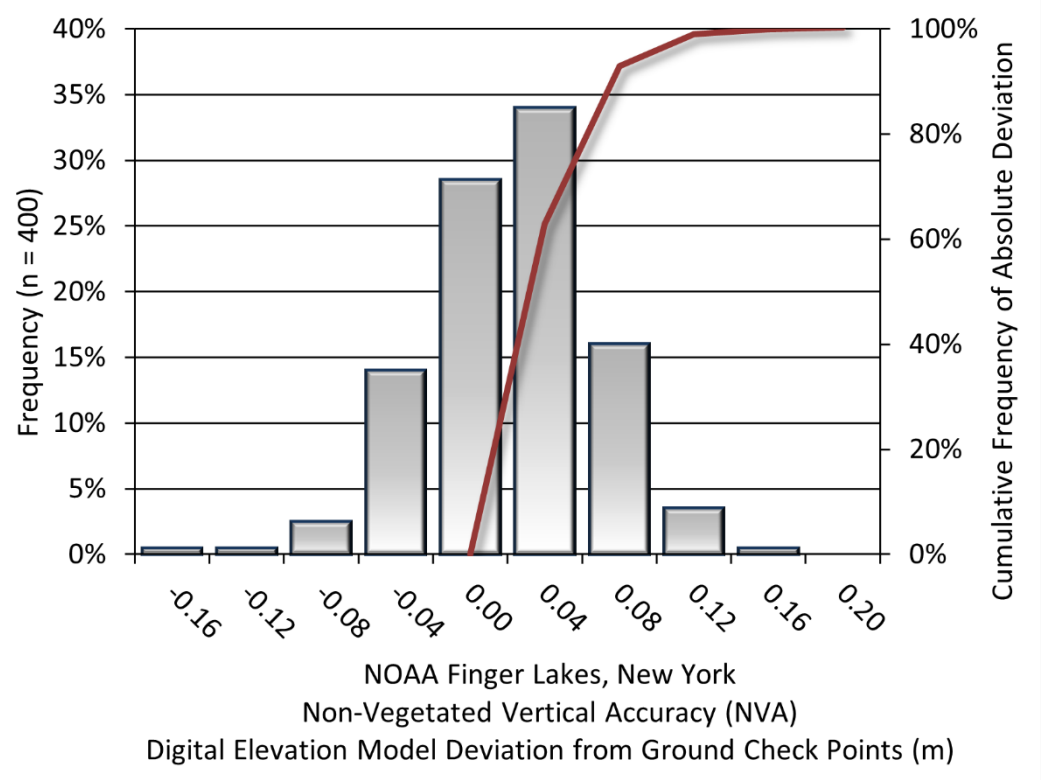

Figure 14: Frequency histogram for lidar bare earth DEM deviation from ground check point values

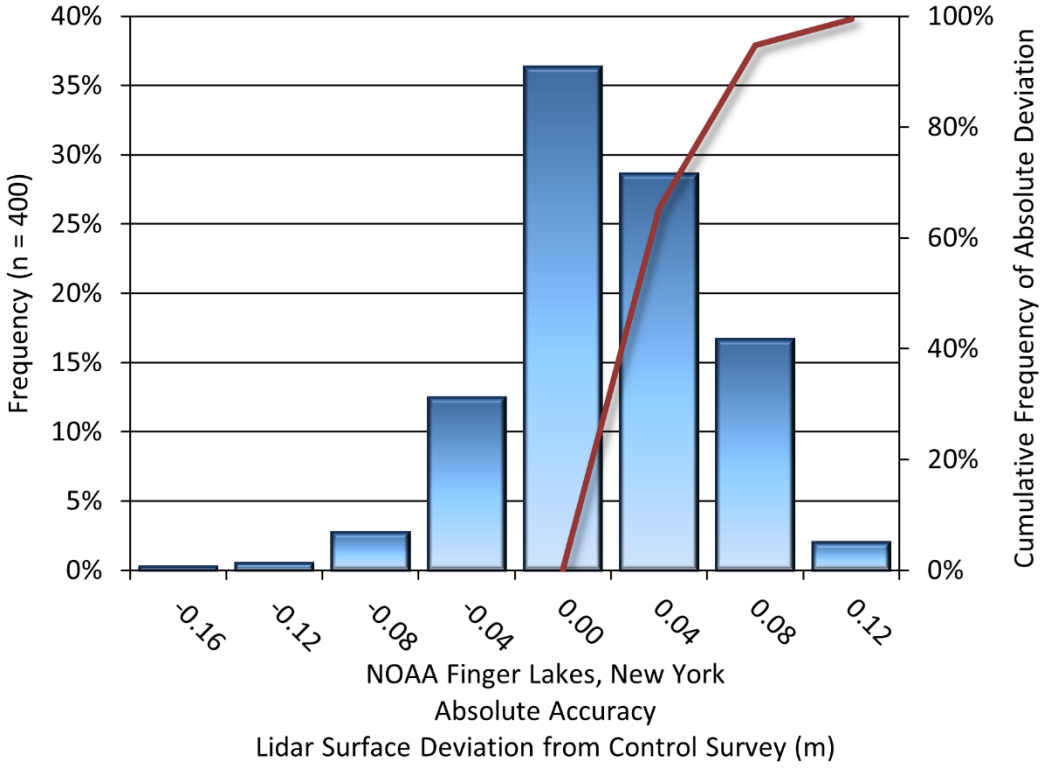

Figure 15: Frequency histogram for lidar surface deviation ground control point values

Lidar Relative Vertical Accuracy

Relative vertical accuracy refers to the internal consistency of the data set as a whole: the ability to place an object in the same location given multiple flight lines, GPS conditions, and aircraft attitudes. When the lidar system is well calibrated, the swath-to-swath vertical divergence is low (<0.10 meters). The relative vertical accuracy was computed by comparing the ground surface model of each individual flight line with its neighbors in overlapping regions. The average (mean) line to line relative vertical accuracy for the NOAA Finger Lakes Lidar project was 0.029 meters (Table 9, Figure 16).

Table 9: Relative accuracy results

Parameter	Relative Accuracy
Sample	460 surfaces
Average	0.029 m
Median	0.025 m
RMSE	0.031 m
Standard Deviation (1σ)	0.011 m
1.96σ	0.022 m

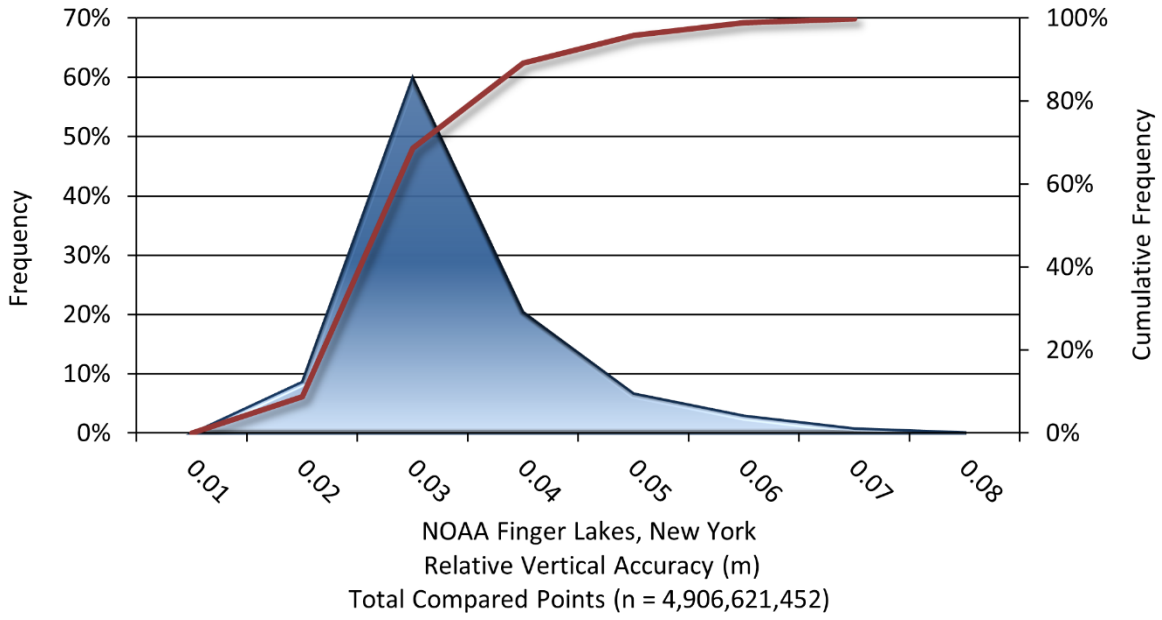

Figure 16: Frequency plot for relative vertical accuracy between flight lines

Lidar Horizontal Accuracy

Lidar horizontal accuracy is a function of Global Navigation Satellite System (GNSS) derived positional error, flying altitude, and inertial navigation system (INS) derived attitude error. The obtained $RMSE_r$ value is multiplied by a conversion factor of 1.7308 to yield the horizontal component of the National Standards for Spatial Data Accuracy (NSSDA) reporting standard where a theoretical point will fall within the obtained radius 95 percent of the time. For the Finger Lakes project, the horizontal accuracy was determined using the IMU/GNSS performance measurements reported by Riegl for the VQ-880-G lidar sensor. Based on a flying altitude of 396 meters, an IMU error of 0.0025 decimal degrees, and a GNSS positional error of 0.05 meters, this project met 0.10 meters horizontal accuracy at the 95% confidence level (Table 10).

Table 10: Horizontal Accuracy

Parameter	Horizontal Accuracy
$RMSE_r$	0.06 m
ACC_r	0.10 m

Figure 17: View looking west over the Oneida Lake in the NOAA Finger Lakes AOI. The image was created from the lidar bare earth model overlaid with the above-ground point cloud and colored by elevation.

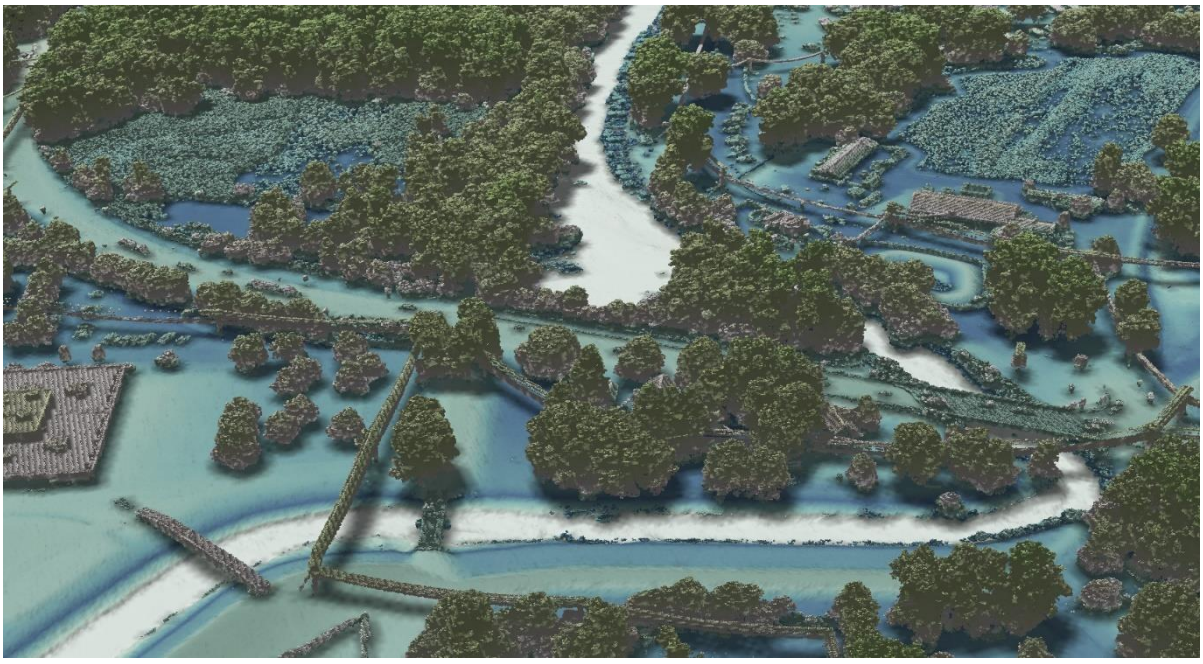

Figure 18: View looking northwest over the Seneca Lake in the NOAA Finger Lakes AOI. The image was created from the lidar bare earth model overlaid with the above-ground point cloud and colored by elevation.

Figure 19: View looking southwest over the Cayuga Lake in the NOAA Finger Lakes AOI. The image was created from the lidar bare earth model overlaid with the above-ground point cloud and imagery and was colored by elevation.

Figure 20: View looking southeast over Lake Champlain in the NOAA Finger Lakes AOI. The image was created from the lidar bare earth model overlaid with the above-ground point cloud and was colored by elevation.

GLOSSARY

1-sigma (σ) Absolute Deviation: Value for which the data are within one standard deviation (approximately 68th percentile) of a normally distributed data set.

1.96 * RMSE Absolute Deviation: Value for which the data are within two standard deviations (approximately 95th percentile) of a normally distributed data set, based on the FGDC standards for Non-vegetated Vertical Accuracy (FVA) reporting.

Accuracy: The statistical comparison between known (surveyed) points and laser points. Typically measured as the standard deviation (sigma σ) and root mean square error (RMSE).

> **Absolute Accuracy:** The vertical accuracy of lidar data is described as the mean and standard deviation (sigma σ) of divergence of lidar point coordinates from ground survey point coordinates. To provide a sense of the model predictive power of the dataset, the root mean square error (RMSE) for vertical accuracy is also provided. These statistics assume the error distributions for x, y and z are normally distributed, and thus we also consider the skew and kurtosis of distributions when evaluating error statistics.
>
> **Relative Accuracy:** Relative accuracy refers to the internal consistency of the data set; i.e., the ability to place a laser point in the same location over multiple flight lines, GPS conditions and aircraft attitudes. Affected by system attitude offsets, scale and GPS/IMU drift, internal consistency is measured as the divergence between points from different flight lines within an overlapping area. Divergence is most apparent when flight lines are opposing. When the lidar system is well calibrated, the line-to-line divergence is low (<10 cm).
>
> **Root Mean Square Error (RMSE):** A statistic used to approximate the difference between real-world points and the lidar points. It is calculated by squaring all the values, then taking the average of the squares and taking the square root of the average.

Data Density: A common measure of lidar resolution, measured as points per square meter.

Digital Elevation Model (DEM): File or database made from surveyed points, containing elevation points over a contiguous area. Digital terrain models (DTM) and digital surface models (DSM) are types of DEMs. DTMs consist solely of the bare earth surface (ground points), while DSMs include information about all surfaces, including vegetation and man-made structures.

Intensity Values: The peak power ratio of the laser return to the emitted laser, calculated as a function of surface reflectivity.

Nadir: A single point or locus of points on the surface of the earth directly below a sensor as it progresses along its flight line.

Overlap: The area shared between flight lines, typically measured in percent. 100% overlap is essential to ensure complete coverage and reduce laser shadows.

Pulse Rate (PR): The rate at which laser pulses are emitted from the sensor; typically measured in thousands of pulses per second (kHz).

Pulse Returns: For every laser pulse emitted, the number of wave forms (i.e., echoes) reflected back to the sensor. Portions of the wave form that return first are the highest element in multi-tiered surfaces such as vegetation. Portions of the wave form that return last are the lowest element in multi-tiered surfaces.

Real-Time Kinematic (RTK) Survey: A type of surveying conducted with a GPS base station deployed over a known monument with a radio connection to a GPS rover. Both the base station and rover receive differential GPS data and the baseline correction is solved between the two. This type of ground survey is accurate to 1.5 cm or less.

Post-Processed Kinematic (PPK) Survey: GPS surveying is conducted with a GPS rover collecting concurrently with a GPS base station set up over a known monument. Differential corrections and precisions for the GNSS baselines are computed and applied after the fact during processing. This type of ground survey is accurate to 1.5 cm or less.

Scan Angle: The angle from nadir to the edge of the scan, measured in degrees. Laser point accuracy typically decreases as scan angles increase.

Native Lidar Density: The number of pulses emitted by the lidar system, commonly expressed as pulses per square meter.

APPENDIX A - ACCURACY CONTROLS

Relative Accuracy Calibration Methodology:

Manual System Calibration: Calibration procedures for each mission require solving geometric relationships that relate measured swath-to-swath deviations to misalignments of system attitude parameters. Corrected scale, pitch, roll and heading offsets were calculated and applied to resolve misalignments. The raw divergence between lines was computed after the manual calibration was completed and reported for each survey area.

Automated Attitude Calibration: All data was tested and calibrated using TerraMatch automated sampling routines. Ground points were classified for each individual flight line and used for line-to-line testing. System misalignment offsets (pitch, roll and heading) and scale were solved for each individual mission and applied to respective mission datasets. The data from each mission were then blended when imported together to form the entire area of interest.

Automated Z Calibration: Ground points per line were used to calculate the vertical divergence between lines caused by vertical GPS drift. Automated Z calibration was the final step employed for relative accuracy calibration.

Lidar accuracy error sources and solutions:

Source	Type	Post Processing Solution
Long Base Lines	GPS	None
Poor Satellite Constellation	GPS	None
Poor Antenna Visibility	GPS	Reduce Visibility Mask
Poor System Calibration	System	Recalibrate IMU and sensor offsets/settings
Inaccurate System	System	None
Poor Laser Timing	Laser Noise	None
Poor Laser Reception	Laser Noise	None
Poor Laser Power	Laser Noise	None
Irregular Laser Shape	Laser Noise	None

Operational measures taken to improve relative accuracy:

Focus Laser Power at narrow beam footprint: A laser return must be received by the system above a power threshold to accurately record a measurement. The strength of the laser return (i.e., intensity) is a function of laser emission power, laser footprint, flight altitude and the reflectivity of the target. While surface reflectivity cannot be controlled, laser power can be increased and low flight altitudes can be maintained.

Reduced Scan Angle: Edge-of-scan data can become inaccurate. The scan angle was reduced to a maximum of ±20° to ±21° from nadir, creating a narrow swath width and greatly reducing laser shadows from trees and buildings.

Quality GPS: Flights took place during optimal GPS conditions (e.g., 6 or more satellites and PDOP [Position Dilution of Precision] less than 3.0). Before each flight, the PDOP was determined for the survey day. During all flight times, a dual frequency DGPS base station recording at 1 second epochs was utilized and a maximum baseline length between the aircraft and the control points was less than 13 nm at all times.

Ground Survey: Ground survey point accuracy (<1.5 cm RMSE) occurs during optimal PDOP ranges and targets a minimal baseline distance of 4 miles between GPS rover and base. Robust statistics are, in part, a function of sample size (n) and distribution. Ground survey points are distributed to the extent possible throughout multiple flight lines and across the survey area.

50% Side-Lap (100% Overlap): Overlapping areas are optimized for relative accuracy testing. Laser shadowing is minimized to help increase target acquisition from multiple scan angles. Ideally, with a 50% side-lap, the nadir portion of one flight line coincides with the swath edge portion of overlapping flight lines. A minimum of 50% side-lap with terrain-followed acquisition prevents data gaps.

Opposing Flight Lines: All overlapping flight lines have opposing directions. Pitch, roll and heading errors are amplified by a factor of two relative to the adjacent flight line(s), making misalignments easier to detect and resolve.